An Improved Method to Estimate Radar Echo Top Height

Valliappa Lakshmanan[1,2], Kurt Hondl[2], Corey K. Potvin[2], David Preignitz[1,2*]

*Corresponding author: V Lakshmanan, 120 David L. Boren Blvd, Norman OK 73072; lakshman@ou.edu

[1]Cooperative Institutute of Mesoscale Meteorological Studies, University of Oklahoma; [2]National Oceanic and Atmospheric Administration / National Severe Storms Laboratory

ABSTRACT

It is demonstrated that the traditional method, in widespread use on NEXRAD and other radar systems, to compute echo top heights results in both under- and overestimates. It is proposed that echo tops be computed by interpolating between elevation scans that bracket the echo top threshold. The traditional and proposed techniques are evaluated using simulated radar samples of a modeled thunderstorm and by sampling a high-resolution Range Height Indicator (RHI) of a real thunderstorm. It is shown that the proposed method results in smaller errors when higher elevation scans are available.

1. Motivation

Radar echo tops have been widely used in meteorology ever since the first weather radars were employed. Applications have ranged from aviation weather forecasting (Evans et al. 2004) and severe weather diagnosis (Held 1978) to gauging the effectiveness of cloud seeding (Goyer 1975). However, the first precise definition of an echo top is difficult to determine since the first uses of radar echo tops seem to have been organic and little remarked upon. Donaldson (1964) noted that the "conventional" echo top is the maximum height of the minimum detectable echo and suggested, citing a private conversation with Dr. David Atlas, that a storm echo top be designated by the maximum height of some standard value of reflectivity.

One problem with this definition of an echo top, as the maximum height at which an echo could occur, arises from side-lobes (Atlas et al. 1963) which can cause the reflectivity value, Z, reported at a particular location to be valid as much as two half-power beamwidths

away. To address this problem, Probert-Jones (1963) devised iterative methods using a set of elevation scans spaced a half-power beam width (hereafter β) apart (what we now term a volume scan) and Donaldson (1964) suggested reducing the receiver gain to suppress side lobes.

This technique, of using a volume scan to determine the maximum elevation angle at which a certain reflectivity threshold is exceeded, is what is now employed operationally on many radar systems. Within NEXRAD, for example, the radar echo top is computed within a volume scan by determining the maximum elevation angle at which dBZ $\geq$ 18 is detected. The echo top height is computed from the elevation angle assuming a 4/3 earth model (Doviak and Zrnic 1993) to account for standard atmospheric refractivity. Rather than use the elevation angle directly, however, the "top" of the beam is used as the echo top height. The top of the radar beam is assumed to occur $\frac{\beta}{2}$ degrees above the nominal elevation angle of the beam. This correction continues to be carried out even though studies as early as Saunders and Ronne (1962) pointed out that the $\frac{\beta}{2}$ correction had no impact on echo top errors.

In spite of the early adoption of radar echo top calculation methods, their limitations were clearly recognized. Radar reflectivity profiles of thunderstorms were described by Donaldson (1961) and Riehl (1977) noted, for example, "clouds may well extend above the upper limits of droplets returning energy to the 10 cm radar." When computing echo tops, therefore, one needs to consider the vertical profile of reflectivity (See Figure 1).

In this paper, we simply reiterate the points made 50 years ago and suggest that the operational computation of echo top heights be modified. We demonstrate that better estimates of echo top heights can be obtained by assuming a locally linear variation in the vertical re-

flectivity profile near the cloud top. Linear interpolation to compute echo tops is not novel: linear interpolation is how echo tops are computed by the Warning Decision Support System – Integrated Information (WDSS-II; Lakshmanan et al. (2007)), by the Corridor Integrated Weather System (Evans et al. 2004) and possibly by other suites of radar algorithms. Thus, for example, in Figure 2, the echo top on the left is the "enhanced" echo top distributed on the NEXRAD Level-III product stream whereas the echo top on the right was computed using WDSS-II from the Level-II NEXRAD data. Even though interpolation to compute echo tops is not new, it has not yet been shown to improve upon the NEXRAD implementation. Demonstrating the advantage of using linear interpolation is the novel contribution of this paper. We hope that the results will prompt revision of the echo top algorithm in the NEXRAD radar products generator and in any other systems where the NEXRAD algorithm is employed.

The rest of this paper is organized as follows. In Section 2, we describe the improved radar echo top method. In Section 3, we demonstrate the method's superiority using a modeled thunderstorm sampled by radars at different ranges. In Section 4, we further demonstrate its performance using real data where the echo top height is known to a high degree of accuracy.

2. Interpolation

Instead of simply finding the highest elevation angle within a volume, or a virtual volume (Lynn and Lakshmanan 2002), where reflectivity exceeds some threshold, the modified algorithm is as follows:

i. Find the maximum elevation angle where reflectivity exceeds the echo top reflectivity threshold. Call this θ_b and the reflectivity value at the elevation Z_b.

ii. If θ_b is not the highest elevation scan in the virtual volume, obtain the reflectivity value at the next higher elevation angle, θ_a, and call it Z_a. If θ_a exists within the virtual volume but Z_a is below the signal-to-noise cutoff, set Z_a =-14 dBZ. This value is chosen because it is the minimum reflectivity value reported by the WSR-88D. Then, the echo top height is given by the height of the radar beam at an elevation angle given by:

$$\theta_T = (Z_T - Z_a)\frac{(\theta_b - \theta_a)}{(Z_b - Z_a)} + \theta_b \tag{1}$$

where Z_T is the threshold value (18 dBZ, for example) used to compute the echo top.

iii. If θ_b is the highest elevation scan available, set $\theta_T = \theta_b + \frac{\beta}{2}$. This condition is met far away from the radar if higher elevation scans have shorter ranges than a base "surveillance" scan and very close to the radar if the highest elevation scan does not sample the top of the cloud. Under these circumstances, θ_T is set to be the top of the beam containing dBZ $\geq Z_T$, i.e., the traditional echo top algorithm is followed when there are no data available from a higher elevation scan.

Linearly interpolating the echo top between the elevation angles that bracket the threshold value of reflectivity is equivalent to finding the elevation angle at which the radar would return 18 dBZ given that the reflectivity at the pulse volumes centered around the two bracketing elevations are known. In other words, this is equivalent to deconvolving the reflectivity values reported by the radar by assuming a Bessel-2 function for the distribution of power density within the beam (Doviak and Zrnic 1993) as long as we make some simplifying as-

sumptions about the reflectivity profile.[1] Because the deconvolution is under-determined, an assumption must be made about the vertical reflectivity profile. If one assumes that the gradient of hydrometeor particle density is constant with height, then it is appropriate to use reflectivity factors (mm^6m^{-3}) in Equation 1. On the other hand, if one assumes that the gradient of the moisture content is constant with height, then it is appropriate to use dBZ values in Equation 1. We report results of interpolating both dBZ and the reflectivity factor, but confine our discussions to the interpolation of dBZ because it was found, empirically, to perform better. Readers interested in the differences between interpolating in dBZ and in mm^6m^{-3} are directed to Lakshmanan (2012).

3. Modeled Thunderstorm and Simulated Radars

A supercell thunderstorm was simulated using the National Severe Storms Laboratory Collaborative Model for Multiscale Atmospheric Simulation (Wicker and Skamarock 2002; Conrad et al. 2006). The simulation proceeded on a 200 × 200 × 20 km domain with 1-km horizontal spacing and vertical spacing increasing from 200 m over the lowest 1 km to 600 m above z = 13 km. The model was integrated over 2 hours using large and small time steps of 4 s and 2/3 s, respectively. A fully dual-moment version of the Ziegler (1985) microphysics

[1]The Bessel-2 function, J_2, has three useful properties in this context: it sums up to 1, $\int J_2(\theta)\theta d\theta = 0$ and when the function is shifted by α, the integral evaluates to α. We seek to find α such that $\int J(\theta-\alpha)Z(\theta)d\theta = Z_T$. By using a Taylor expansion for $Z(\theta)$ and the above properties of the Bessel function, it can be seen that $\alpha = (Z_T - Z_a)\frac{(\theta_b-\theta_a)}{(Z_b-Z_a)}$ when $Z(\theta)$ is linear in θ, and $\alpha = (log(Z_T) - log(Z_a))\frac{(\theta_b-\theta_a)}{(log(Z_b)-log(Z_a))}$ when $log(Z(\theta))$ is linear in θ.

scheme (Mansell et al. 2010) was used. The simulation exhibits all of the critical features of real supercells, including a deep, rotating updraft (mesocyclone), rear- and forward-flank downdrafts, and outflow-induced gust fronts and baroclinic zones.

Synthetic reflectivity observations of the simulated supercell were computed from the model reflectivity Z at t = 40 min using a slightly modified version of the technique of Wood et al. (2009). This technique emulates the power-weighted averaging of reflectivities (and radial velocities) of scatterers within a Gaussian radar beam. Earth curvature and standard atmospheric beam refraction are also represented. The emulated radar was positioned at successively greater distances east of the simulated supercell. The radar β and effective β (See Doviak and Zrnic (1993) pages 193-197) were set to 0.89^o and 1.39^o, respectively. Samples were collected every 250 m in range and 0.5^o in azimuth using the NEXRAD VCP 11. The results of this process are shown in Figure 3.

The "true" echo top height was computed from the model data in its native Cartesian coordinate system. Because the model's vertical resolution is very high, the echo top height was simply set to the maximum nominal (staggered) height at which the radar reflectivity exceeded 18 dBZ, i.e., we did not perform any interpolation for determining the "true" echo top heights.

At each pixel in the horizontal grid for which there was a finite echo top height, the error was computed as the difference between the echo top height computed from the simulated radar data, $h_{computed}$, and the true echo top height, h_{truth}, obtained from the high-resolution model data:

$$e_h = h_{computed} - h_{truth} \tag{2}$$

The distribution of errors is shown in Figure 4. The thick line shows the median error while the extent of the box indicates the first and third quartiles. In addition, the Mean Absolute Error (MAE) in the echo top estimate (in km) is reported for each method. All the statistics are computed using only locations where the true echo top is greater than zero. The median error and the MAE are reported rather than the Mean Square Error (MSE) or Root Mean Square Error (RMSE) because the median and MAE are more resistant to outlier effects. Taking the first box plot, it can be seen that when the radar is situated 100 km away from the center of the storm, the traditional method results in underestimates of the echo top height (note that the median error is negative indicating that the technique is biased towards underestimation). When dBZ values are interpolated, the median error becomes zero. It can be noted that the median error coincides with the 25th percentile for the traditional method, thus indicating that high negative errors (i.e., gross underestimates) are very frequent. On the other hand, when interpolating dBZ values, the 75th percentile and the median error coincide (at zero), indicating that overestimates are extremely rare. There remain cases of underestimation, but these are far fewer than in the traditional method. In other words, the improvement of the proposed method over the traditional method comprises reduction in the bias. When interpolating Z values, both underestimates and overestimates are equally likely since the median value is equally spaced from the 25th and 75th percentiles. When the radar is situated 150 km away, the median error from both methods is zero, but the new method reduces the variance of the echo top errors. When the value of Z is interpolated, it is seen that the median error and the 75th percentile of the errors coincides, indicating that the large positive errors are very frequent.

The proposed method improves upon the traditional method by utilizing data from the

elevation scan above the scan with reflectivity greater than 18 dBZ. When the radar is so far away that the beams overshoot the top of the storm (the 200 km range in Figure 4) or so near that the top of the storm is not sampled (the 50 km range), there is no improvement using the proposed method.

4. Comparing with High-Resolution RHI

While modeled thunderstorms are useful for precisely evaluating echo top errors and examining their behavior with increasing range from the radar, it is also useful to demonstrate improvements on real reflectivity data. To do this, we used a high-resolution Range Height Indicator (RHI) scan as truth and computed the echo tops by sampling the RHI using a typical NEXRAD VCP. It was thus possible to quantify how the echo top height is improved, albeit on only a few cases.

The high resolution RHI data were collected using the National Weather Radar Testbed Phased Array Radar (NWRT PAR; Zrnic et al. (2007)). The NWRT PAR consists of a single antenna array capable of sampling a 90 degree sector in both azimuth and elevation angle. The effective beam width at boresight is 1.5 degrees with the beam width increasing away from boresight by a factor $1.5/\cos(a)$, where a is the angle from boresight. Because the antenna is tilted vertically by 10 degrees, for a traditional NEXRAD VCP with an elevation angle range of 0.5 to 19.5 degrees, the angles from boresight range from -9.5 to +9.5 degrees, resulting in a maximum beam width of 1.52 degrees at the larger off-boresight angles.

The volume scan chosen followed the typical NEXRAD VCP elevation angle range of 0.5 to 19.5 degrees. However, an elevation angle interval of 0.25 degrees was used, resulting in

77 distinct elevation cuts. In addition, a single azimuth position was sampled resulting in a total scan time of approximately two seconds.

The high-resolution RHI obtained is shown in Figure 5. The "true echo top" was derived from the RHI using the traditional NEXRAD algorithm (i.e., the echo top was defined to be $\frac{\beta}{2}$ above the central elevation angle of the highest beam with dBZ $\geq$ 18 dBZ). This RHI was then sampled using the elevation angles in NEXRAD's VCP 11 by selecting the closest elevation angle in the high-resolution RHI. From the sampled VCP, the echo tops were computed using the traditional and proposed (interpolation) methods. The true echo top height is shown on the left panels of Figure 6 while the distributions of errors when the echo top is computed from the sampled VCP are shown in the right panels Figure 6. It can be seen that interpolating in dBZ reduces the spread of the errors. Consequently, the mean absolute errors obtained using the interpolation method are lower than those obtained using the traditional method. The process was carried out on a few days where there were storms within range of the PAR. The results consistently exhibited a lower variance of error when dBZ values were interpolated to estimate the echo top height.

As expected, and similar to the case of the simulated thunderstorms, the reduction in the spread of echo top error is most dramatic when the storms are about 100 km from the radar (the middle row of Figure 6). When there are storms 200 km away from the radar, as in the third row, interpolation can not mitigate the error by much because the available elevation scans in VCP 11 do not sample the cloud top. Consequently, the underestimate of echo top height can be as much as 10 km.

5. Summary

This note demonstrated the advantage of using linear interpolation of dBZ values bracketing an echo top threshold to compute echo top heights. If the thunderstorm is situated such that the top of the cloud is sampled by the radar, then interpolation reduces the bias and the variance in the echo top estimation error. It is hoped that these results will prompt revision of the echo top algorithm in the NEXRAD radar products generator and in any other systems where the NEXRAD algorithm is employed to compute echo tops. We also recommend that any conclusions, forecasting techniques and decision criteria that were arrived at through the analysis of NEXRAD echo tops products be reexamined in light of this study.

Acknowledgements

Funding for V. Lakshmanan and D. Preignitz was provided by NOAA/Office of Oceanic and Atmospheric Research under NOAA-University of Oklahoma Cooperative Agreement NA11OAR4320072, U.S. Department of Commerce. C. Potvin was supported by a National Research Council Postdoctoral award at NSSL.

We would like to thank Ben Baranowski, Chris Porter, Brent Shaw and Beth Clarke of Weather Decision Technologies (WDT) for posing the question – of why WDSS-II echo top heights were different from those in the Level-III stream – that prompted this note.

Finally, we wish to thank Don Burgess, Rodger Brown and Vincent Wood of NSSL for their helpful comments during the preparation of this manuscript.

REFERENCES

Atlas, D., K. Browning, R. Donaldson, and H. Sweeney, 1963: Automatic digital radar reflectivity analysis of a tornadic storm. *J. of Appl. Meteor.*, **2**, 574–581.

Conrad, M., D. Stensrud, and L. Wicker, 2006: Effects of upper-level shear on the structure and maintenance of strong quasi-linear mesoscale convective systems. *J. Atmos. Sci.*, **63**, 1231–1252.

Donaldson, R., 1961: Radar reflectivity profiles in thunderstorms. *J. Meteor.*, **18**, 292–305.

Donaldson, R., 1964: A demonstration of antenna beam errors in radar reflectivity patterns. *J. Appl. Meteo.*, **3 (5)**, 611–623.

Doviak, R. and D. Zrnic, 1993: *Doppler Radar and Wea. Observations*. 2d ed., Academic Press, Inc.

Evans, J., K. Caruson, M. Wolfson, M. Robinson, E. Ducot, and B. Crowe, 2004: Improving convective weather operations in highly congested airspace with the corridor integrated weather system (CIWS). *11th Conf. on Aviation, Range and Aerospace Meteor.*, Hyannis, MA, Amer. Meteor. Soc., P5.4.

Goyer, G., 1975: Time-integrated radar echo tops as a measure of cloud seeding effects. *J. Appl. Meteo.*, **14 (7)**, 1362–1365.

Held, G., 1978: The probability of hail in relation to radar echo heights on the south african highveld. *J. Appl. Meteo.*, **17 (6)**, 755–762.

Lakshmanan, V., 2012: Image processing of weather radar reflectivity data: Should it be done in z or dbz? *Elec. J. Severe Storms Meteo.*, **7 (3)**, 1–4.

Lakshmanan, V., T. Smith, G. J. Stumpf, and K. Hondl, 2007: The warning decision support system – integrated information. *Wea. Forecasting*, **22 (3)**, 596–612.

Lynn, R. and V. Lakshmanan, 2002: Virtual radar volumes: Creation, algorithm access and visualization. *21st Conf. on Severe Local Storms*, San Antonio, TX, Amer. Meteor. Soc.

Mansell, E., C. Ziegler, and E. Bruning, 2010: Simulated electrification of a smal thunderstorm with two-moment bulk microphysics. *J. Atmos. Sci.*, **67**, 171–194.

Probert-Jones, J., 1963: The distortion of cumulonimbus precipitation observed by radar. Tech. Rep. Tech. Note No. 13, Imperial College of Science and Technology, 21 pp., London. Available via http from gatekeeper.dec.com/pub/DEC/SRC/research-reports/abstracts/src-rr-124.html.

Riehl, H., 1977: Vertical distribution of energy transfer and radar echo tops in the equatorial trough zone. *Monthly Wea. Review*, **105 (2)**, 230–231.

Saunders, P. and F. Ronne, 1962: A comparison between the height of cumulus clouds and the height of radar echoes received from them. *J. Appl. Meteo.*, **1**, 296–302.

Wicker, L. and W. Skamarock, 2002: Time-splitting methods for elastic models using forward tim schemes. *Mon. Wea. Rev.*, **130**, 2088–2097.

Wood, V., R. Brown, and D. Dowell, 2009: Simulated WSR-88D velocity and reflectivity signatures of numerically modeled tornadoes. *J. Atmos. Oceanic Technol.*, **26**, 876–893.

Ziegler, C., 1985: Retrieval of thermal and microphysical variables in observed convective storms. *J. Atmos. Sci.*, **42**, 1487–1509.

Zrnic, D., et al., 2007: Agile beam phased array radar for weather observations. *Bull. Amer. Meteor. Soc.*, **88**, 1753–1766.

List of Figures

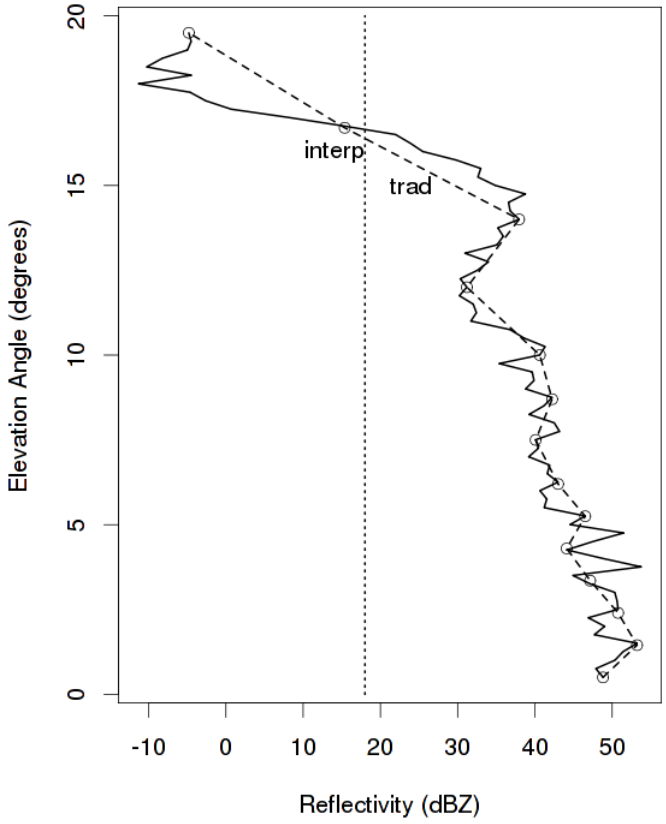

FIG. 1. Determining the echo top height by interpolating the vertical profile of reflectivity between elevation scans that bracket the echo top threshold. The vertical profile shown was obtained at a range of 40 km from the NWRT PAR on June 21, 2012. The profile sampled at the elevation angles of VCP 11 of the WSR-88D is shown by the points, and linear interpolation of this profile by the dashed line. In this case, the traditional method of obtaining the 18 dBZ echo top ("trad" in the figure) is an underestimate whereas the interpolated height ("interp" in the figure) is much closer to the true value.

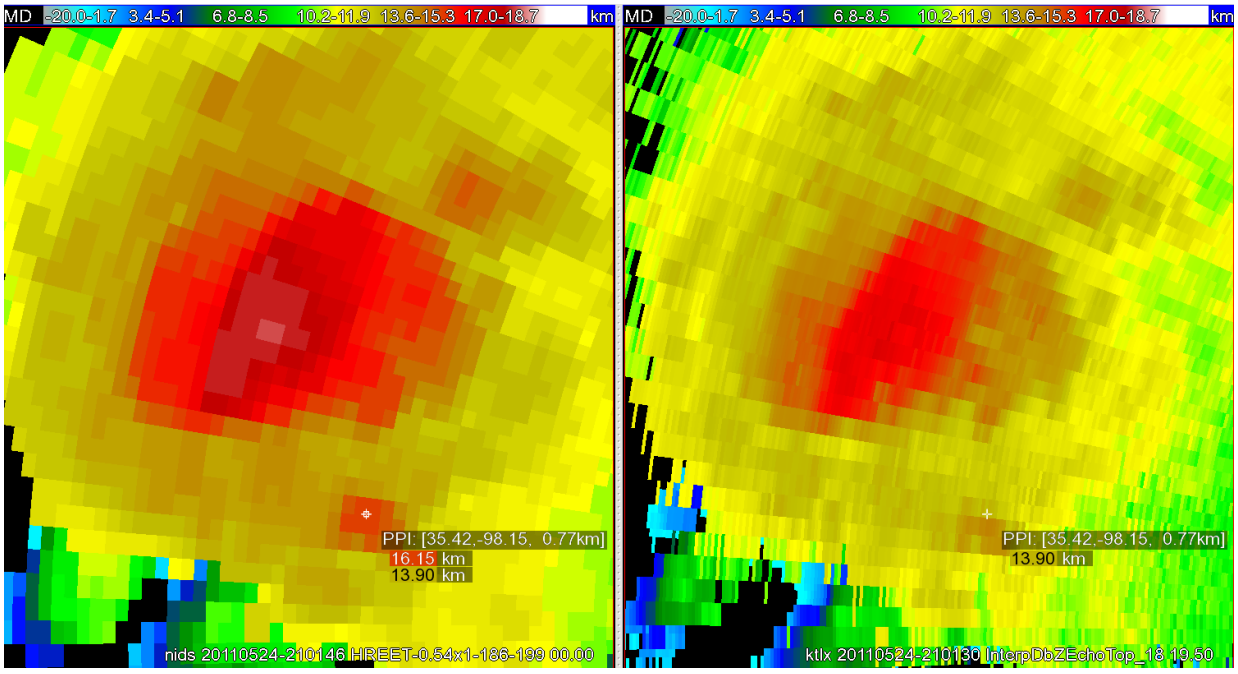

FIG. 2. Data from a May 24, 2011 storm over Oklahoma. The echo top on the left is the "enhanced" echo top distributed on the Level-III product stream whereas the echo top product on the right is generated using WDSS-II from the Level-II NEXRAD stream. Note that the difference in the echo top height at the cursor location is more than 2 km (16.2 vs. 13.9 km).

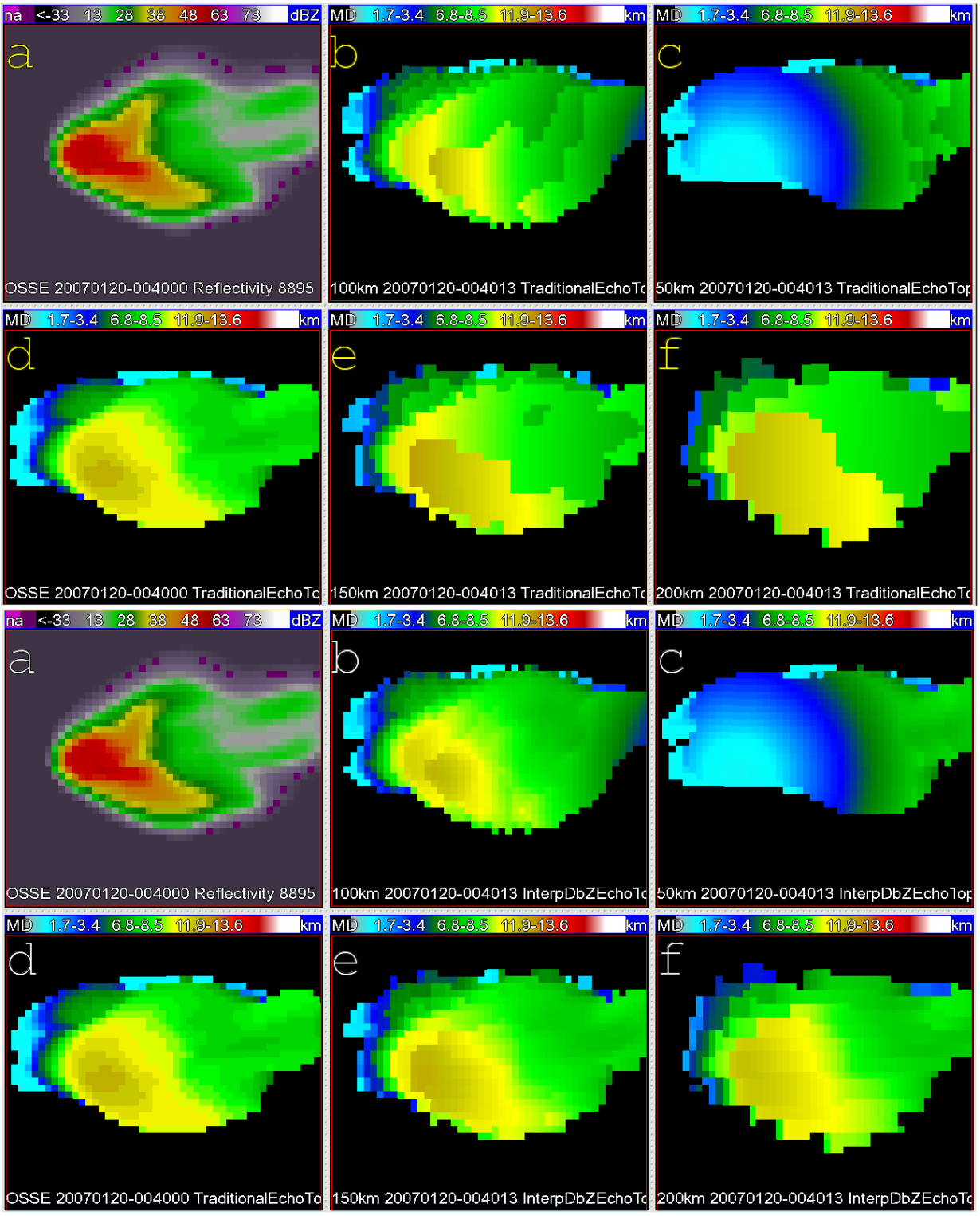

FIG. 3. The six panels on the top illustrate the computation of echo top heights the traditional way whereas the six panels on the bottom illustrate the use of interpolation to compute the echo top. In both cases, the six panels are: (a) radar reflectivity from the model at around 9 km above the ground; (b) echo top computed with a radar simulated to lie 100 km away from the center of the storm; (c) radar simulated to lie 50 km away; (d) the "true" echo top computed in the model's Cartesian coordinate system; (e) radar simulated to lie 150 km away; (f) radar simulated to lie 200 km away.

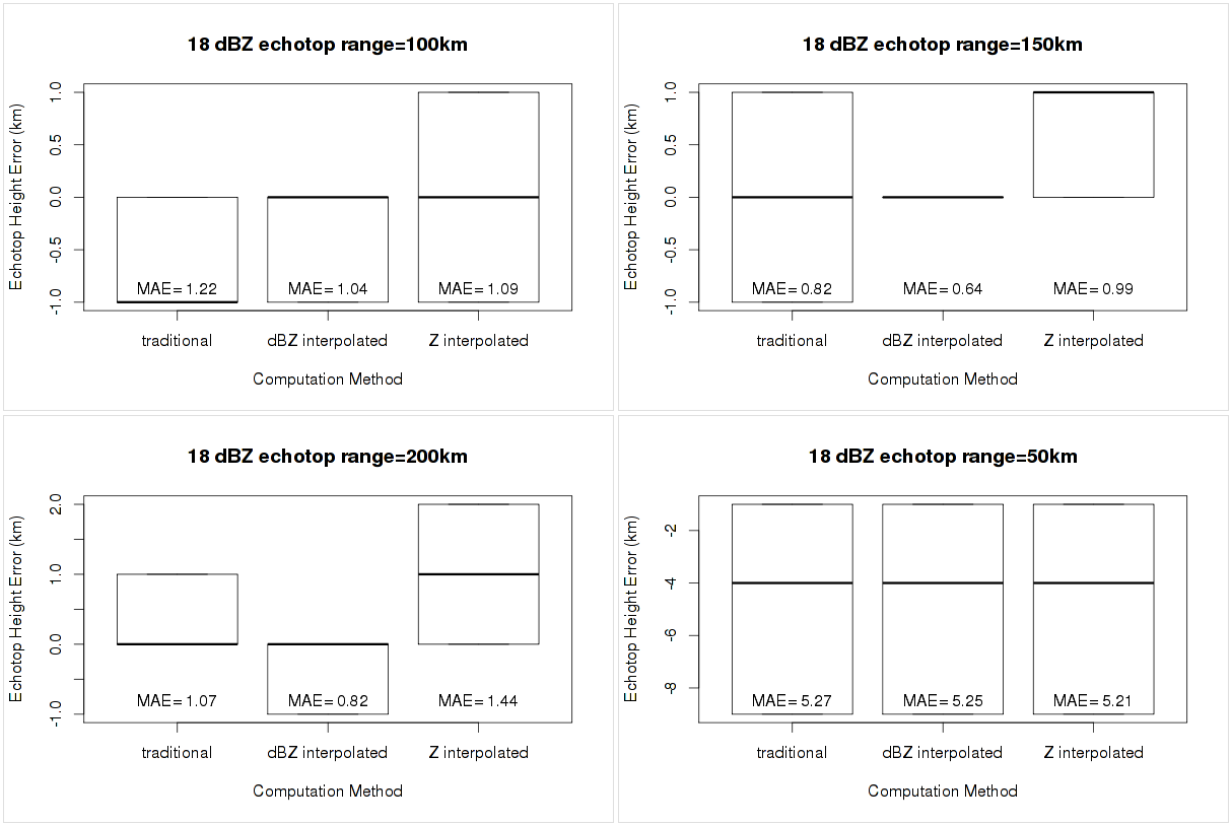

FIG. 4. Distribution of errors in the 18 dBZ echo top when the modeled thunderstorm is at different distances from the radar. Each plot shows the median error (dark line) and the first and third quartiles (box) as well as the Mean Absolute Error (MAE) in km. Interpolating dBZ values between elevation scans results in lower echo top errors at mid-ranges.

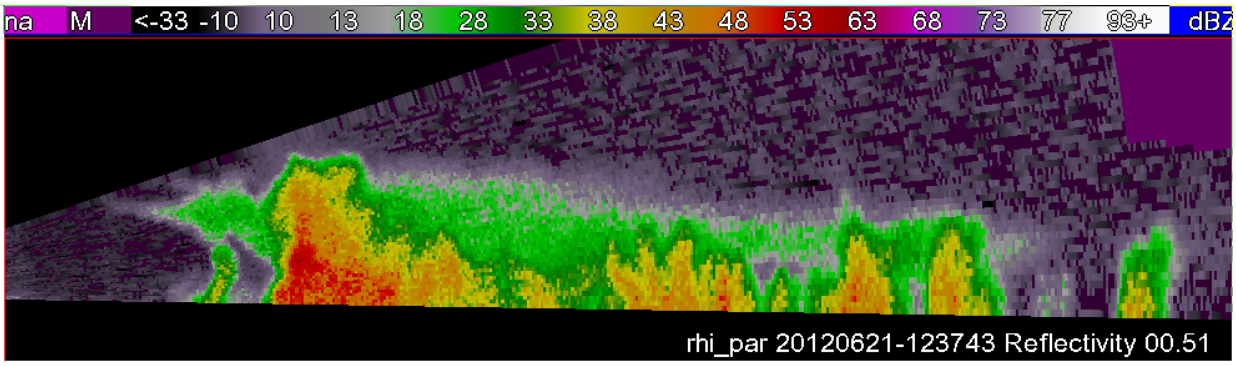

FIG. 5. High-resolution (in the vertical) RHI scan from NWRT PAR on June 21, 2012. For height and range information, please see the first panel of Fig. 6.

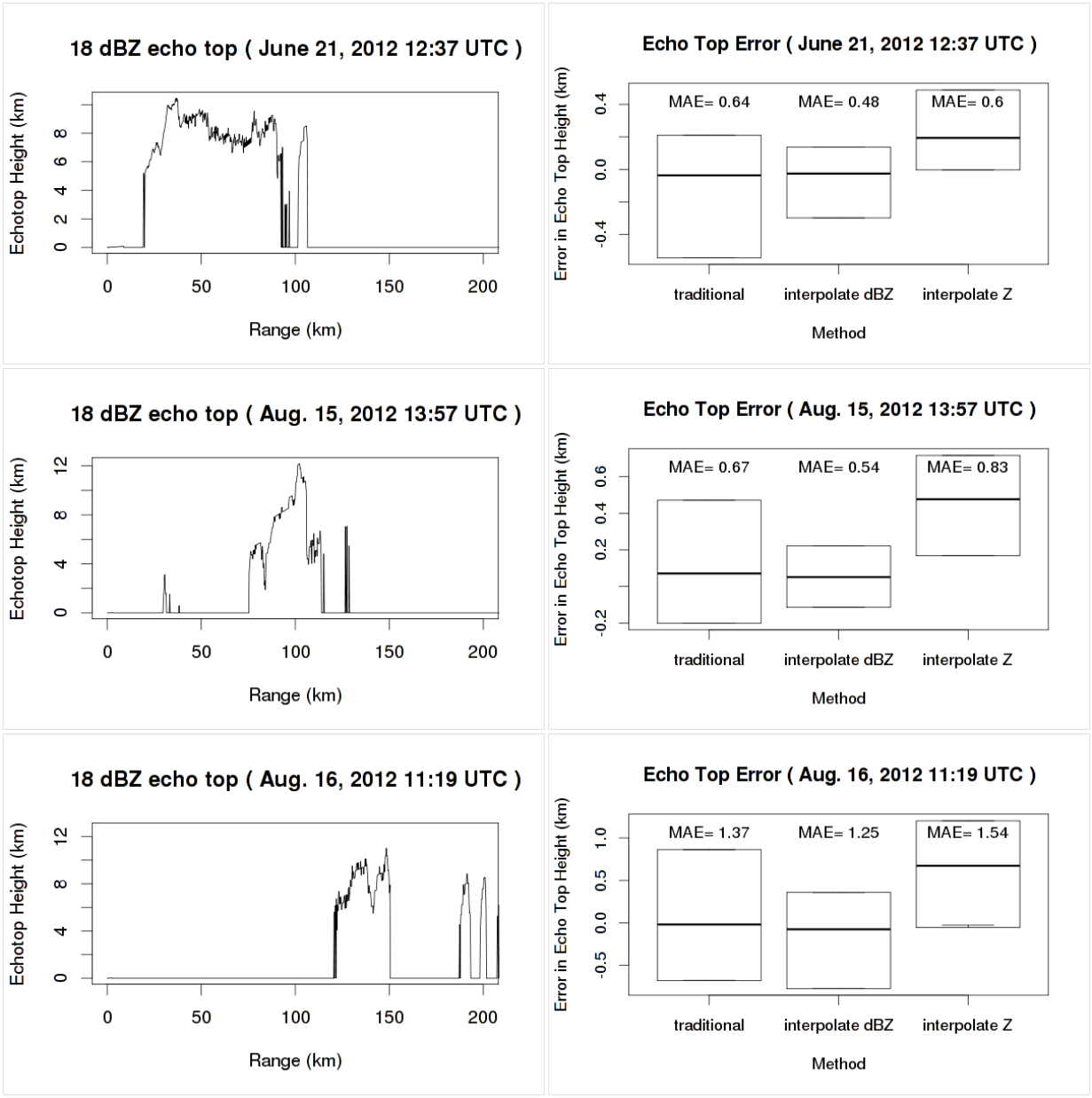

FIG. 6. Left panels show the true echo tops obtained using the NWRT PAR on several days in 2012. The right panels show the errors in the 18 dBZ echo top when computing using the traditional NEXRAD method and by interpolating reflectivity values between beams that bracket the 18 dBZ threshold value.